

Magnetic anisotropy and intergrain interactions in $L1_0$ CoPt(1 1 1)/Pt(1 1 1)/MgO(1 0 0) PLD granular films with tilted easy axes

G Varvaro¹, E Agostinelli¹, S Laureti¹, A M Testa¹,
J M García-Martin², F Briones² and D Fiorani¹

¹ ISM-CNR, Istituto di Struttura della Materia, Area della Ricerca di Roma1,
Via Salaria km 29.500, CP 10-00016 Monterotondo Scalo, Roma, Italy

² Instituto de Microelectrónica de Madrid, IMM-CNM-CSIC, Isaac Newton 8,
28760 Tres Cantos, Madrid, Spain

E-mail: gaspere.varvaro@ism.cnr.it

Received 21 January 2008, in final form 4 March 2008

Published 19 June 2008

Online at stacks.iop.org/JPhysD/41/134017

Abstract

The magnetic properties of tilted easy axis $L1_0$ CoPt(1 1 1)/Pt(1 1 1)/MgO(1 0 0) film, deposited by pulsed laser deposition, were investigated by magnetization angular dependence measurements and magnetic force microscopy (MFM). The room temperature anisotropy constant, evaluated measuring the in-plane variation of transverse magnetization under a rotating magnetic field, is $K_1 = 5 \times 10^6 \text{ erg cm}^{-3}$. The domain structure, observed by MFM, consists of decoupled single domain grains, unlike the maze-like structure usually observed for similar systems. This was confirmed by the analysis of dc demagnetization and isothermal remanence magnetization curves, which provided evidence of predominant magnetostatic interactions.

1. Introduction

$L1_0$ FePt and CoPt films, due to their high uniaxial magnetocrystalline anisotropy (for single crystals $K_u = 6.6 \times 10^7 \text{ erg cm}^{-3}$ and $4.0 \times 10^7 \text{ erg cm}^{-3}$, respectively [1, 2]) and chemical stability, have been widely investigated in recent years in view of their application as perpendicular magnetic recording media [3–5] with the potential of reaching Tb/in² densities. However, one of the main drawbacks of perpendicular recording is the high sensitivity of the switching field to the magnetic easy axis (EA) distribution, which contributes to the media noise [6]. It was found that a much better tolerance of the EA distribution could be achieved in so-called tilted media, where the easy axis of the grains is tilted to an optimal 45° angle with respect to the surface normal [7–9].

As reported in the literature [10, 11], the required tilting of the magnetic easy axis is commonly obtained employing

an oblique deposition geometry, although the oblique grains microstructure usually implies increased roughness and stress and shape anisotropy effects [12].

In a previous paper [13] we have reported on the structural properties of epitaxial $L1_0$ CoPt(1 1 1)/Pt(1 1 1)/MgO(1 0 0) films grown by conventional frontal pulsed laser deposition (PLD), and the study of the magnetic easy axes space arrangement by angular remanence measurements. It consisted of four out-of-plane easy axes forming an angle of $\sim 36^\circ$ with respect to the film plane, with mutually orthogonal in-plane projections (figure 1(a)). To our knowledge, such an arrangement has never been reported in the literature before. The crystal structure of $L1_0$ CoPt cell with (1 1 1) growth orientation is schematically illustrated in figure 1(b). Four different CoPt variants could arise from the two platinum in-plane orientation variants that form when Pt(1 1 1) grows onto MgO(1 0 0), and their presence could explain the observed magnetic properties.

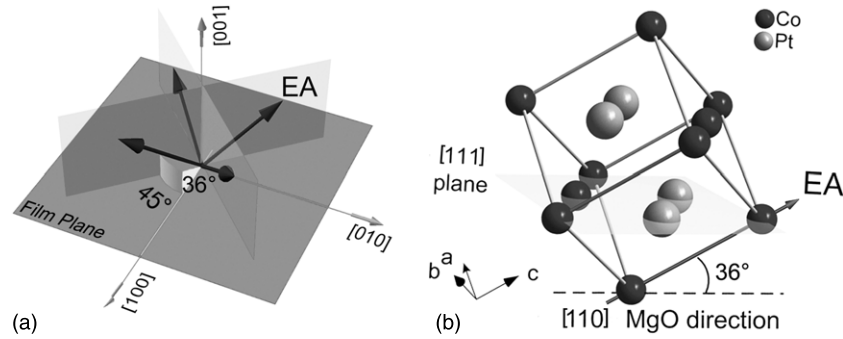


Figure 1. Schematic illustration of the four tilted EA model (a) and of the $L1_0$ CoPt cell with (111) growth orientation (b). The spatial reference system is given by the MgO(100) crystallographic axes.

In this paper, we report on further investigations of anisotropy properties, domain configuration and intergrain interactions in this system.

2. Experimental

Film depositions were performed in HV condition ($P_{\text{dep}} = 1 \times 10^{-7}$ mbar) by PLD using a pulsed KrF (248 nm) excimer laser at an energy fluence $F = 3 \text{ J cm}^{-2}$. The pulse repetition rate was 10 Hz with a pulse duration of 17 ns. The substrate and the target were assembled in a frontal geometry at 55 mm reciprocal distance. A carousel with Pt and composite CoPt targets were used to sequentially deposit the two different layers. A very thin Pt(111) underlayer (thickness $\sigma \sim 4$ nm) was deposited at $T = 573$ K for a duration time $t = 2'$ on MgO(100) [14] to favour the epitaxial growth of the magnetic layer along the $[111]$ direction. CoPt films were then deposited at $T = 873$ K for a duration time $t = 7'$ and annealed at the same temperature in order to avoid the presence of metastable phases and to favour the transition from the magnetically soft fcc to the magnetically hard fct phase. Films of the $L1_0 \text{ Co}_x\text{Pt}_{1-x}$ alloy ($x \sim 0.5$, thickness $\sigma \sim 15$ nm), which presented a strong uniaxial anisotropy along the c -axis, were obtained [13], as deduced from structural characterization by energy dispersive x-ray diffraction and magnetic measurements. In particular the tetragonal cell grew as schematically illustrated in figure 1(b). The magnetic properties were studied at room temperature using a commercial vectorial vibrating sample magnetometer (VSM model 10—ADE Technologies), equipped with a rotating electromagnet. The anisotropy constant was evaluated measuring the transverse magnetization M_{\perp} (projection of M along the axis normal to the vector H) while rotating a saturating magnetic field in the film plane, from 0° to 360° . The resulting torque τ is the product HM_{\perp} and is related to the material anisotropy constant [15]. In order to get information on the nature of the intergrain interactions, isothermal remanence magnetization (IRM) and dc demagnetization (DCD) remanence curves [16, 17] were collected by applying a maximum perpendicular magnetic field of 19 kOe.

Atomic force microscopy (AFM) and magnetic force microscopy (MFM) images were obtained using a NanotecTM microscope operating in non-contact dynamic mode at ambient

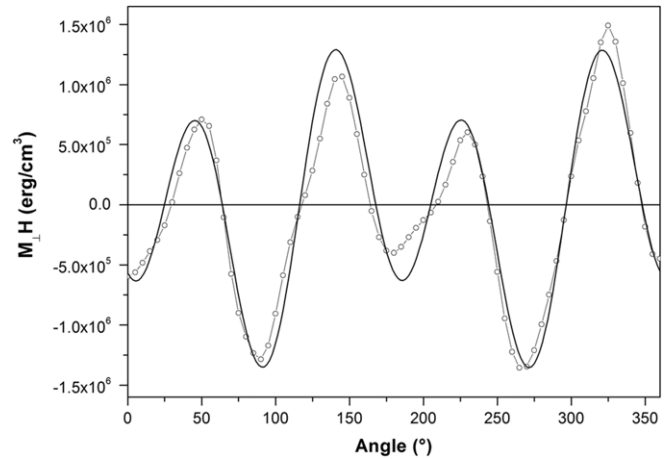


Figure 2. (—○—) In-plane torque curve measured with an applied field of 15 kOe; (—) fitting curve: $y = A \sin ax + B \sin bx$.

conditions. For MFM, the tip scanned at a constant lift height above the sample, typically 50 nm, and the phase shift, proportional to the force gradient, was measured. The probes were commercial Si cantilevers from NanosensorsTM (force constant in the $3\text{--}5 \text{ N m}^{-1}$ range, resonant frequency in the $65\text{--}80$ kHz range) with a pyramidal tip at the end, and were home coated, by means of sputtering, with a Cr/Co/Cr trilayer. The thickness of this coating was carefully tailored in order to produce tips with coercivity high enough to remain stable during the scans, i.e. not to be remagnetized by the sample stray field once magnetized in an electromagnet along the direction of the pyramid axis.

3. Results and discussion

3.1. Anisotropy measurements

In order to estimate the room temperature anisotropy constant K_1 , we have studied the anisotropy along the film plane, assuming a pseudo cubic biaxial symmetry, which comes from the orthogonal projections of the four magnetocrystalline easy axes on this plane. For a system with such a complex geometrical arrangement of the easy axis, like ours, a more accurate evaluation of the anisotropy constants would require measurements in many different intersecting planes [18]; such investigation is still in progress.

For a single domain system, the variation of the angle between the applied field H and the magnetization M can be calculated by minimizing the magnetic free energy.

The torque $\tau = -\partial E/\partial\vartheta$, considering the cubic biaxial symmetry, can be written as (1)

$$\tau = \frac{K_1}{4} \sin(4\vartheta) = HM \sin(\alpha - \vartheta), \quad (1)$$

where K_1 is the anisotropy constant, $M \sin(\alpha - \vartheta)$ corresponds to the transverse magnetization M_{\perp} , ϑ is the angle between the EA and M and α is the angle between the EA and H . The measurements (figure 2) were carried out at $H = 15$ kOe and a K_1 value of 4×10^6 erg cm $^{-3}$ was then extracted by the fitting. Considering that the easy axes form an angle of 36° with respect to the film plane, a value of 5×10^6 erg cm $^{-3}$ was calculated, which is consistent with the value of magnetocrystalline anisotropy of the L1 $_0$ phase. Moreover, this value is comparable to the value of the anisotropy constant obtained from the coercive field measured along one of the easy directions ($K = \frac{1}{2}M_s H_c$). The weaker uniaxial contribution, evidenced by the different amplitude

of the modulation, was not due to sample misalignment and its origin is still under investigation. Indeed, neither angular remanence magnetization [13] nor angular coercivity measurements (figure 3) gave evidence of the existence of an additional uniaxial anisotropy. Actually, a conventional torque measurement implies a geometry where the easy axis lies in the same plane where H is rotated. This simple geometry cannot be obtained in our tilted system for all four axes simultaneously. For this reason, the measurements performed in-plane showed anomalies which could arise in the absence of co-planarity between H and the four easy axes. Nevertheless, the approximation still provides a value of K_1 , in reasonable agreement with the literature.

3.2. AFM/MFM imaging

The surface topography (AFM) and the magnetic force gradient map (MFM), which is proportional to the magnetic pole density [19, 20], were acquired simultaneously in non-contact dynamic mode, in ambient conditions (figures 4(a) and (b), respectively). Before measurements, samples were demagnetized in an alternating magnetic field along the direction perpendicular to the film plane.

As shown in the AFM image, the film is characterized by a granular structure where grains of similar height (20 nm) and straight edges appear well separated from each other, with an individual average area of the upper surface of about 10^4 nm 2 . In the MFM image, the dark and the bright regions are due to the North and South magnetic poles at the surface, respectively. Taking into account the 3D easy axes arrangement previously described, these poles can be ascribed to magnetization lying along one easy axis pointing in the inward (South) or outward (North) directions with respect to the sample surface. The majority of the grains exhibited uniform magnetic contrast, i.e. they are single domain, as for instance the four grains along the

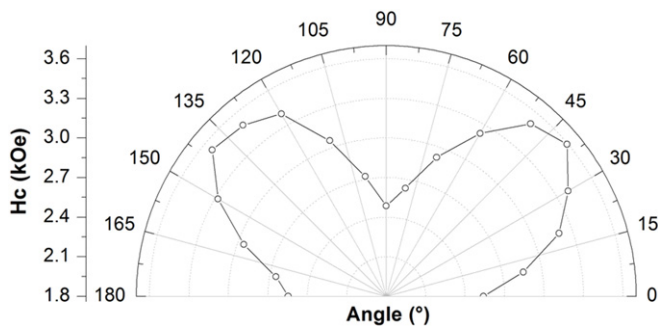


Figure 3. In-plane angular coercivity dependence ($H_{\max} = 19$ kOe).

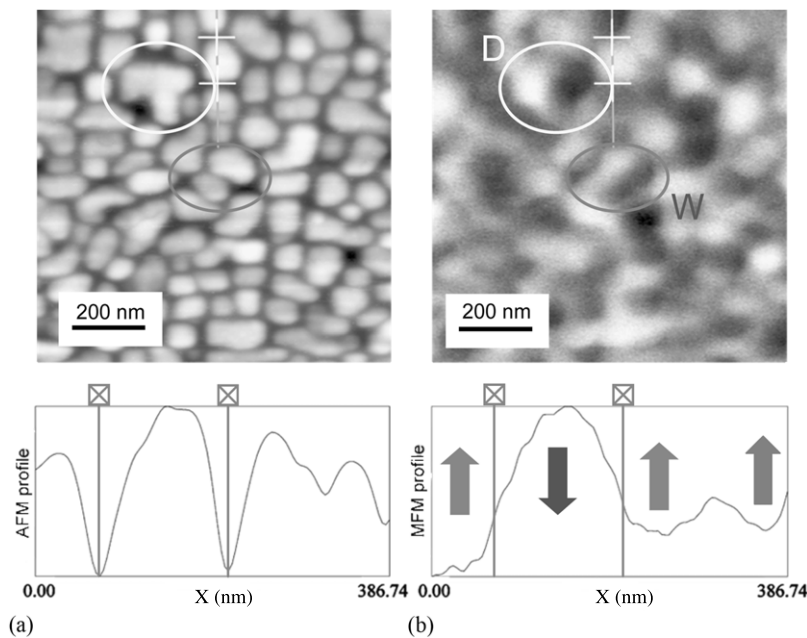


Figure 4. Correlation between (a) the topography of CoPt film obtained by AFM imaging and (b) the magnetic domain structure from MFM, the two measurements being acquired simultaneously. The two profiles are related to the same physical line on the film, and the arrows indicate the magnetization component in the out-of-plane direction in these grains.

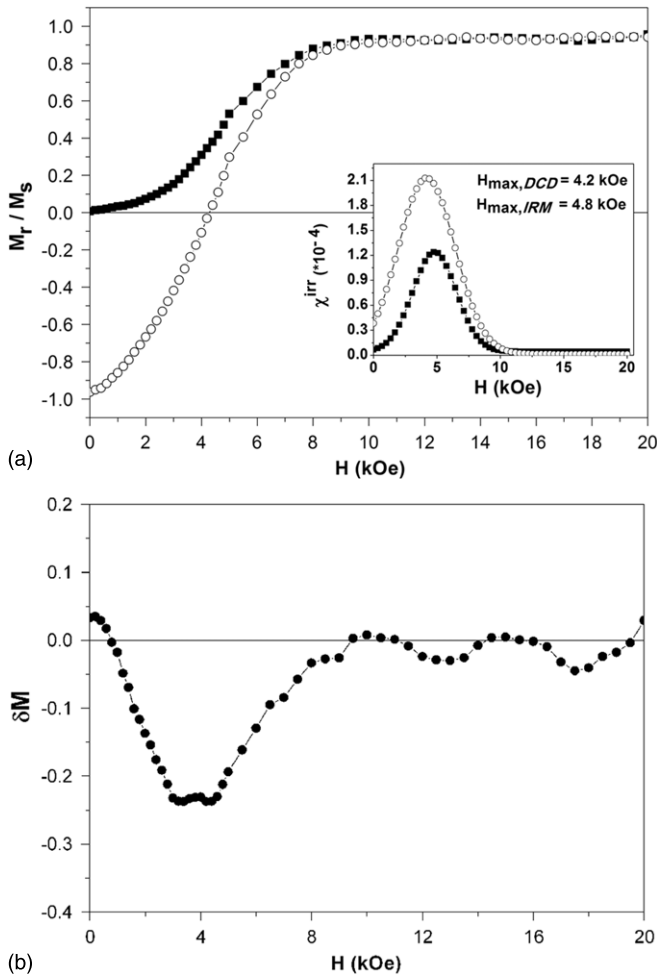


Figure 5. (a) Comparison between the IRM (—■—) and DCD (—○—) remanence curves. In the inset the field derivative is reported. (b) δM plot derived from the remanence measurements.

lines indicated in the AFM and MFM images whose profiles are depicted below them (lower part of figure 4): the second grain (located between the two marks) exhibited a bright contrast, whereas the first, the third and the fourth ones exhibited a dark contrast. A few grains, usually of bigger size, exhibited a non-uniform contrast with different regions that can be ascribed to different magnetic domains: this is the case of the grain labelled D in the MFM image exhibiting two domains that give rise to bright (on the left) and dark (on the right) contrast. Finally, in a few cases, some domains larger than the size of a single grain were observed, such as those labelled W in the image, and they are probably due to the existence of a weak exchange coupling between adjacent grains in those zones. In summary, the domain configuration is different from the typical maze-like structure usually found in $L1_0$ thin films where each magnetic domain contains several grains [21].

3.3. Magnetic remanence measurements

In order to get a deeper insight into the intergrain interactions present in our samples, a series of magnetization remanence curves was collected applying the magnetic field perpendicular to the sample surface (figure 5(a)). In particular, for the

IRM curves, the sample was initially demagnetized through successive minor loops, while in the DCD measurements the sample was first saturated in a high negative field (-19 kOe). The same sequence of progressively higher applied fields up to 19 kOe was used for both measurements, in order to easily correlate the two curves.

By differentiating the two remanence curves with respect to the field it is possible to obtain the irreversible susceptibility χ^{irr} that represents a map of the switching field distribution in both magnetizing (DCD) and demagnetizing modes (IRM). For an ideal non-interacting system, the two differentiated curves should overlap, with a factor of 2 in the height of the $dM_{r,IRM}/dH$ relative to the $dM_{r,DCD}/dH$ curve derived from the Wohlfarth relation (2) [16]

$$M_{r,DCD} = 1 - 2M_{r,IRM}. \quad (2)$$

In a real system, any deviation from this relationship can be attributed to the effect of interactions as proposed by Kelly *et al* [17], who expressed the parameter δM as (3)

$$\delta M = M_{r,DCD} - [1 - 2M_{r,IRM}]. \quad (3)$$

This parameter, which is zero in the absence of interactions, is therefore a direct measure of deviations from the non-interacting case. Positive values of δM are due to interactions promoting the magnetized state (exchange interactions), whereas negative values of δM are due to demagnetizing interactions (e.g. dipole–dipole interactions).

The results of the remanence measurements showed the quasi-ideal behaviour of a non-interacting system, as the fields at which the χ^{irr} curves show a maximum are very close ($H_{max,DCD} = 4.2$ kOe and $H_{max,IRM} = 4.8$ kOe) and $\chi_{max,IRM}^{irr} = 1.8\chi_{max,DCD}^{irr}$ (inset of figure 5(a)). The negative δM value (figure 5(b)) indicates the predominance of demagnetizing magnetostatic interactions. The absence of significant intergrain exchange coupling can be attributed to the nearly isolated grain morphology of the magnetic layer obtained by using a very thin and granular Pt underlayer as a template.

4. Conclusions

We have studied the anisotropy properties, the domain configuration and intergrain interactions in PLD grown $L1_0$ CoPt films with four tilted easy axes. The room temperature anisotropy constant K_1 has been estimated measuring the in-plane angular dependence of the transverse magnetization under a magnetic field and the value obtained (5×10^6 erg cm^{-3}) is consistent with the anisotropy of the $L1_0$ phase.

AFM measurements showed that the films are composed of separated grains, and the MFM analysis showed that the majority of the grains exhibited a single domain state.

The δM plot analysis of the remanence curves provided evidence of behaviour close to what was expected for an ideal non-interacting system. The negative δM maximum indicated that magnetostatic interactions are mainly present, thus tending to stabilize a demagnetized state in the system. The isolated

grain morphology for the magnetic layer is attributed to the discontinuous morphology of the Pt underlayer used as a template.

Acknowledgments

The research work was supported by CNR in the framework of the CNR-CSIC scientific cooperation agreement. The authors would like to thank D Petrelli and E Patrizi for technical assistance in PLD deposition and magnetic measurements, respectively.

References

- [1] Varanda L C, Jafelicci M Jr and Imaizumi M 2007 *J. Appl. Phys.* **101** 123918
- [2] Shima E, Oikawa K, Fujita A, Fukamichi K and Ishida K 2005 *Appl. Phys. Lett.* **86** 112515
- [3] Iwashaki S and Nakamura Y 1977 *IEEE Trans. Magn.* **13** 1272
- [4] Judy J 2005 *J. Magn. Magn. Mater.* **287** 16
- [5] Weller D, Moser A, Folks L, Best M E, Lee W, Toney M F, Schwickert M, Thiele J U and Doerner M F 2000 *IEEE Trans. Magn.* **36** 10
- [6] Zou Y Y, Wang J P, Hee C H and Chong T C 2003 *Appl. Phys. Lett.* **82** 2473
- [7] Wang J P 2005 *Nature Mater* **4** 191
- [8] Gao K Z and Bertram H N 2002 *IEEE Trans. Magn.* **38** 3675
- [9] Wang J P, Zou Y Y, Hee C H, Chong T C and Zheng Y F 2003 *IEEE Trans. Magn.* **39** 1930
- [10] Tanahashi K, Hosoe Y and Futamoto M 1996 *J. Magn. Magn. Mater.* **153** 265
- [11] Zheng Y F, Wang J P and Ng V 2002 *J. Appl. Phys.* **91** 8007
- [12] Klemmer T and Pelhos K 2006 *Appl. Phys. Lett.* **88** 162507
- [13] Varvaro G, Agostinelli E, Laureti S, Testa A M, Generosi A, Barbara P and Rossi Albertini V Study of magnetic easy axis 3D-arrangement in L1₀-CoPt(1 1 1)/Pt(1 1 1)/MgO(1 0 0) tilted system for perpendicular recording *IEEE Trans. Magn.* at press
- [14] Scavia G, Agostinelli E, Laureti S, Varvaro G, Paci B, Generosi A, Rossi Alberini V, Kaciulis S and Mezzi A 2006 *J. Phys. Chem. B* **110** 5529
- [15] Armelles G, Costa-Kramer J L, Martin J I, Anguita J V and Vicent J L 2000 *Appl. Phys. Lett.* **77** 2039
- [16] Wohlfarth E P 1958 *J. Appl. Phys.* **29** 595
- [17] Kelly P E, O'Grady K, Mayo P I and Chantrell R W 1989 *IEEE Trans. Mag.* **MAG-25** 3881
- [18] Abelmann L, Kambersky V, Lodder C and Popma T J A 1993 *IEEE Trans. Magn.* **29** 3022
- [19] Hubert A, Rave W and Tomlinson S L 1997 *Phys. Status Solidi B* **204** 817
- [20] Garcia-Martin J M, Thiaville A, Miltat J, Okuno T, Vila L and Piraux L 2004 *J. Phys. D: Appl. Phys.* **37** 965
- [21] Gehanno V, Marty A, Gilles B and Samson Y 1997 *Phys. Rev. B* **55** 12552